

MINERALOGICAL AND MORPHOLOGICAL STUDY OF LUNAR CRATER MOSTING USING DATASETS FROM RECENT LUNAR MISSIONS. Aurobindo Kumar Basantaray, Mamta Chauhan, Ramdayal Singh, Sumit Pathak, Satadru Bhattacharya and Prakash Chauhan, Space Applications Centre, Indian Space Research Organisation, Ahmedabad – 380 015, India (ram@sac.isro.gov.in).

Introduction: Morphological progression of an impact crater follows as its size increases and complex craters are characterised by a centrally protruding dome surrounded by relatively flat topography produced by breccia filling, crater rim and marginal collapse terraced zones [1]. In spite of their formation in similar environment and with relatively simple mineralogy, lunar complex impact craters exhibit diverse morphology as well as mineral distribution depending upon various factors such as angle, time, velocity of impact, post-modification changes etc [e.g, 2]. Therefore, observation and analysis of morphological features and mineral distribution can provide insights into their geological evolution through time.

The present study is mineralogical and morphological analysis of the crater Mosting (0.7°S-5.9°W) having a characteristic polygonal shape, triangular edged rim flaps and floral patterned flows at the centre. It is ~26 km diameter crater located (Fig. 1a) near the south-eastern fringe of Mare Insularum.

Data used and methods: For mineralogical analysis hyperspectral data from Chandrayaan-1 Moon Mineralogy Mapper (M^3) have been used having wide spectral range (~460-3000nm) for evaluating important mafic minerals [3]. Photometrically and thermally corrected Level-2 data products are used [4]. For morphological analysis high-resolution data from LROC-NAC (~0.5 m/px) have been used [5]. LRO Mini-RF Circular Polarization Ratio (CPR) images [6] have been used to study the surficial physical properties of the crater. In order to differentiate the single bounce, double bounce and randomly-polarized backscatter in the study area m-chi decomposition [7] has also been carried out. For determining the rock abundance LRO-Diviner radiometer data acquired from 14Aug.2009 to 22 May 2014 is used. It has three spectral filters near 8 μm , channels 6, 7 and 8 with full width half maximum of 13-23, 25-41 and 50-100 μm [8].

Results and discussions: To identify the locations of mineral outcrops a false color composite (FCC) mosaic area have been generated using orbital strips of M^3 scenes (Fig.1b). The FCC shows few patches of mafic exposures in the shades of pink and green along its north-northwest side, along crater rim and also mafic exposures in the shades of pink and green along

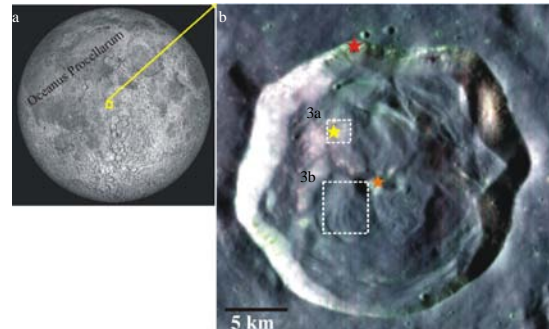


Figure 1. (a) Location of crater Mosting on the Moon (b) FCC image generated from M^3 datasets (R=930nm, G=1249nm and B=2137nm). The stars shows the location of spectra collection.

the central peaks. Individual spectra from the region are then evaluated for detection of major mafic mineral phases that exist in the study site based on the diagnostic absorption features of the major mafic minerals [9,10,11]. Results are presented in Figure 2 with the representative spectra of important minerals in the area. The spectral signatures show the presence of high-ca-pyroxene (HCP) and low-ca pyroxene (LCP) occurring along the rim and central peak along with Mg-spinels present in NW crater floor and rims (Fig. 2a). The spinels that are characterized on the basis of their single absorption feature near 2000-nm are indicative of Mg-spinel [12]. Besides, the 2000-nm feature is showing a longward shift in some of the spectra collected (band centre 2317 nm) indicating the presence of Cr-spinels. In Mg-spinel, the band minima wavelength position occurs shortward of 2100 nm while in Cr-spinel it arises beyond 2100 nm due to the interactions between the octahedral and tetrahedral cations through their shared oxygens [12,13].

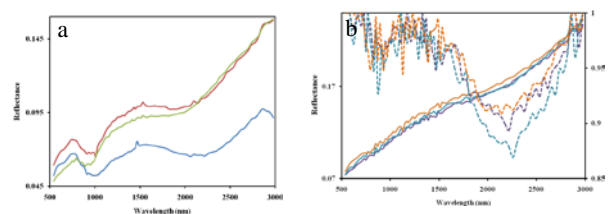


Figure 2. Representative spectras of (a) HCP and LCP collected from red and orange star, Fig.1b and (b) spinels collected from area marked by yellow star, Fig. 1b.

In high-resolution images, the crater Mosting shows highly degraded inner terraced walls, two small central mounds at the centre and a peculiar floral patterned flows at the crater floor. The overall surface appears smooth with a few scattered clast concentrations from where minerals are identified (Fig. 3a). It appears that the flows are guided by underlying structure (Fig. 3b). Rock concentration derived from the binned diviner channel 6 to 8 radiance dataset [14] are shown in Figure 4 and it is clear that the rock abundance is higher over SE portion, over terraced inner wall and over a small central hill where it ranges upto 0.04. Radar observation shows that the area is characterized by overall low Circular Polarization Ratio (CPR) values (Fig. 4a) indicating radar dark area suggestive of scattering from terrain having fine materials. The m-chi decomposition [7] image has been generated covering parts of the crater, in which the floor of the crater appears as green and the adjacent area blue. The blue regions correspond to surface scattering whereas green pixels are indicative of volume scattering. The blue areas therefore could possibly correspond to clast/boulder-poor surfaces. The central peak region appears whitish with some pink dots, which indicates a mixture of surface, volume and double-bounce with dominant surface cum volume scattering.

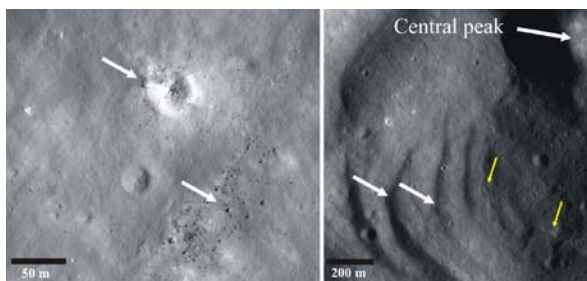


Figure 3. Subsets of LROC-NAC image M192996354LC showing the area marked in Fig. 1b. (a) Few clasts present at the edge of a flow and near a crater (b) SW part of crater floor with characteristic flow pattern.

Conclusion: From the present study it is concluded that the central part of the crater floor is dominated by clast/boulder-poor regolith materials. Rock abundance in the form of boulder clusters is prominent in the central and SW portion of the crater. The detected mafic minerals correspond to either earlier ejecta material, underlying material exposed by later cratering or the clast leftover near the edge of the impact melt flows. Further study related to age determination needs to be carried out in order understand its evolution over time.

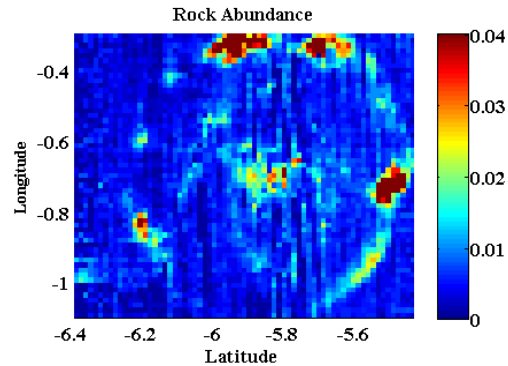


Figure 4. Rock abundance map of Mosting crater.

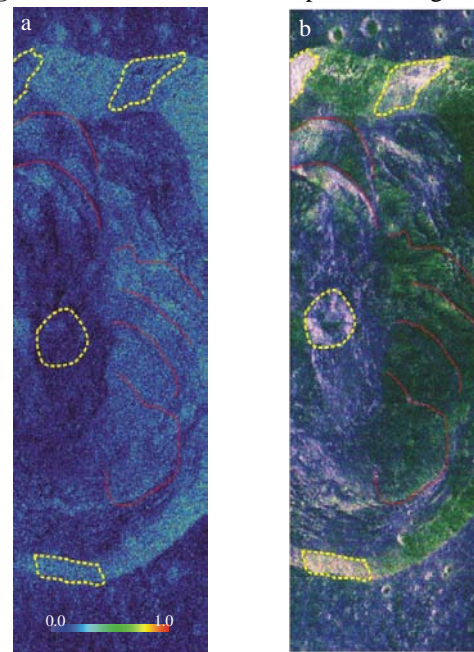


Figure 5. (a) CPR and (b) m-chi decomposition images showing the areas with large rock abundance (demarcated with yellow dotted lines) and typical pattern of the flows (red lines) on the crater floor.

References: [1] Pike, R. J. (1976) *LPI*, 700-702. [2] Hale, W. and Head, J.W. (1979) *LPS X*, 2623-2633. [3] Boardman J. et al. (2011) *JGR* 116, E00G14. [4] Green R. O. et al. (2011) *JGR* 116, E00G19. [5] Robinson M. S. et al. (2010) *Space Sci. Rev.* 150, 81-124. [6] Nozette S. et al. (2010) *Space Sci. Rev.* 150, 285-302. [7] Raney R. K. et al. (2012) *JGR* 117, E00H21. [8] Paige D. A. (2010) *Space Sci. Rev.* 150, 125-160. [9] Burns, R. G. (1993) *Cambr. Univ. Press*, New York, p. 551. [10] Cloutis E. A. and Gaffey M. J. (1991) *JGR* 96, 22809-22826. [11] Klima R. L. et al. (2007) *Meteorit. Planet. Sci.* 42, 235-253. [12] Cloutis E. A. et al. (2004) *Meteorit. Planet. Sci.* 39, 545-565. [13] Farmer V. C. (1974) *Mineral. Soc.*, 183-204. [14] Bandfield J. L. (2011) *JGR* 116, E00H02.